

Polarization effects in the quasi - elastic $(p, 2p)$ reaction with the nuclear S - shell protons at 1 GeV

O. V. Miklukho, A. Yu. Kisselev, D. A. Aksenov, G. M. Amalsky,
V. A. Andreev, S. V. Evstiukhin, O. Ya. Fedorov, G. E. Gavrilov,
A. A. Izotov, L. M. Kochenda, M. P. Levchenko,
D. A. Maysuzenko, V. A. Murzin, D. V. Novinsky,
A. N. Prokofiev, A. V. Shvedchikov, V. Yu. Trautman,
S. I. Trush, A. A. Zhdanov

B.P.Konstantinov Petersburg Nuclear Physics Institute, Gatchina, Russia

The polarization of the secondary protons in the $(p, 2p)$ reaction with the S -shell protons of nuclei ^4He , ^6Li , ^{12}C , ^{28}Si , ^{40}Ca was measured at 1 GeV unpolarized proton beam. The spin correlation parameters C_{ij} for the ^4He and ^{12}C targets also were for the first time obtained as well. The polarization measurements were performed by means of a two-arm magnetic spectrometer, each arm of which was equipped with the multiwire-proportional chamber polarimeter. This experiment was aimed to study a modification of the proton-proton scattering matrix in the nuclear medium.

Comments: 28 pages, 7 figures, 6 tables, Submitted to the journal "Physics of Atomic Nuclei"

Category: Nuclear experiment (nucl-ex)

1 Introduction

There were some speculations on modifications of nucleon and meson masses and sizes, and of meson-nucleon coupling constants, and, as consequence, of a nucleon-nucleon scattering matrix in nuclear medium [1-6]. These speculations were motivated by a variety of theoretical points of view, including the renormalization effects due to strong relativistic nuclear fields, deconfinement of quarks, and partial chiral symmetry restoration.

This work is a part of the experimental program in the frame of which the medium-induced modifications of the nucleon-nucleon scattering amplitudes are studied at PNPI synchrocyclotron with 1 GeV proton beam [7-13]. The intermediate-energy quasi-free ($p, 2p$) reaction is a good experimental way to study such effects, since in the first approximation this reaction can be considered as a proton-proton scattering in the nuclear matter. Usage of S -shell protons (with zero orbital momentum) is preferred because interpretation of obtained data in this case is essentially simplified since the effective polarization is not involved [14]. The polarization observables in the reaction are compared with those in the elastic pp scattering. In our exclusive experiment a two-arm magnetic spectrometer is used, the shell structure of the nuclei being evidently distinguished. To measure polarization characteristics of the reaction, each arm of the spectrometer was equipped with the multiwire-proportional chamber polarimeter.

In early PNPI-RCNP experiment [10], the polarizations P_1 and P_2 of both secondary protons from the ($p, 2p$) reactions at 1 GeV with the $1S$ -shell protons of the nuclei ${}^6\text{Li}$, ${}^{12}\text{C}$ and with the $2S$ -shell protons of the ${}^{40}\text{Ca}$ nucleus has been measured at the nuclear proton momenta close to zero. The polarization observed in the experiment, as well as the analyzing power A_y in the

RCNP experiment at the 392 MeV polarized proton beam [15, 16], drastically differed from that calculated in the framework of non-relativistic Plane Wave Impulse Approximation (PWIA) and of spin-dependent Distorted Wave Impulse Approximation (DWIA) [17], based on free space proton-proton interaction. This difference was found to have a negative value and increases monotonously with the effective mean nuclear density $\bar{\rho}$ [15]. The latter is determined by an absorption of initial and secondary protons in nucleus matter. The observed inessential difference between the non-relativistic PWIA and DWIA calculations pointed out only to a small depolarization of the secondary protons because of proton-nucleon rescatterings inside a nucleus. All these facts strongly indicated a modification of the proton-proton scattering amplitudes due to the modification of the main properties of hadrons in the nuclear matter.

Later, the result of the experiment with the ^4He target broke the mentioned above dependence of a difference between the experimental polarization values and those calculated in the framework of the PWIA on the effective mean nuclear density $\bar{\rho}$ [11]. The difference for the ^4He nucleus proved to be close to that for the ^6Li nucleus. This evidently contradicts to the elastic proton-nucleus scattering experiment. According to the experiment, the ^4He nucleus has the largest mean nuclear density. On the other hand, the mentioned above deviation from the PWIA keeps to be a monotonous function of the S -shell proton binding energy E_s for all investigated nuclei. It is possible that in the light nuclei at least (with atomic number $A < 12$), where the nuclear matter is strongly heterogeneous, the value of $\bar{\rho}$ does not properly reflect the scale of the nuclear medium influence on the properties of the nucleon-nucleon interaction, and the value of E_s may also be a measure of this influence. The important feature of the experiment with the ^4He nucleus

was a possibility to see the medium effect without any contribution from the multi-step processes (for instance, from the $(p, 2pN)$ reactions). These processes could take place when there were nucleons of outer shells as in other nuclei. Therefore they could not also be an origin of the systematic difference between the polarizations P_1 and P_2 clearly obtained for the first time in the experiment [11].

Here we present the polarization data for the reaction with the nuclei ^4He , ^6Li , ^{12}C (1*S*-shell) and ^{40}Ca nucleus (2*S*-shell). These data were obtained by averaging the results of our early experiments [10,11] and the results of the new measurements performed after upgrade of the spectrometer electronics. In the experiments the polarization was measured with much better statistical accuracy for the nuclei ^4He , ^{12}C . We also present new data on the polarization in the reaction with the 1*S*-shell protons of the ^{28}Si nucleus. The 1*S*-state of the ^{28}Si nucleus has the larger value of the mean proton binding energy E_s (50 MeV) in comparison with that of the ^{12}C nucleus (35 MeV).

Due to the new fast electronics CROS-3 of the spectrometer [18], the experimental program was extended to measure the spin correlation parameters C_{ij} in the $(p, 2p)$ reaction with nuclei. The useful counting rate of the reaction drastically drops with increasing the nucleus atomic number due to an absorption of the initial and secondary protons in the nucleus matter. We measured these parameters in the reaction with the light nuclei ^4He and ^{12}C . The main interest was concentrated on measuring the spin correlation parameter C_{nn} since its value is the same in the center-of-mass and laboratory systems. Besides, this parameter is not distorted by the magnetic fields of the two-arm spectrometer because of the proton anomalous magnetic moment [19]. Since the polarization and the spin correlation parameter C_{nn} are expressed differently through the scattering matrix elements [6], the

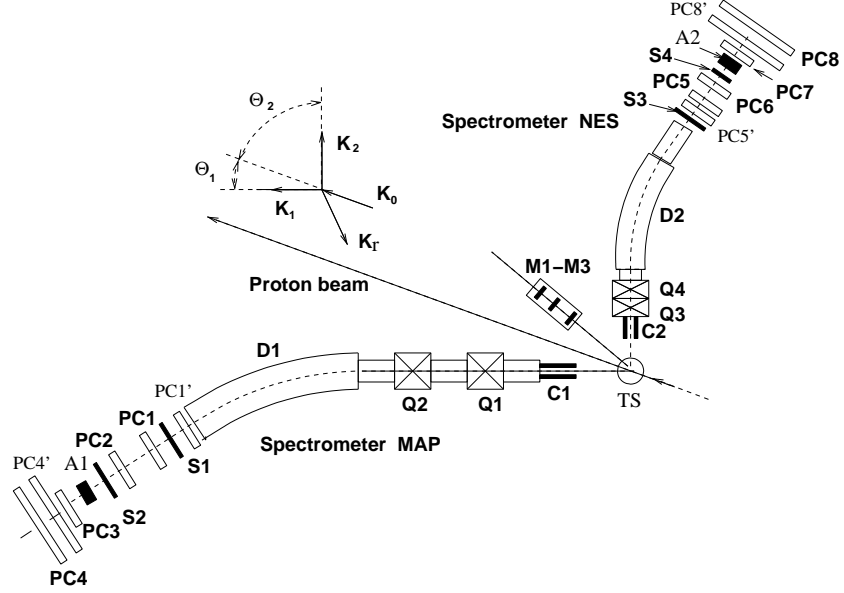


Figure 1: The experimental setup. TS is the target of two-arm spectrometer; $Q1 \div Q4$ are the magnetic quadrupoles; $D1$, $D2$ are the dipole magnets; $C1$, $C2$ are the collimators; $S1 \div S4$ and $M1 \div M3$ are the scintillation counters; $PC1 \div PC4$, $PC1'$, $PC4'$ ($PC5 \div PC8$, $PC5'$, $PC8'$) and $A1$ ($A2$) are the proportional chambers and the carbon analyzer of the high-momentum (low-momentum) polarimeter, respectively. The kinematics for the $(p, 2p)$ reaction is shown.

measurement of both these polarization observables can give more comprehensive information about a modification of the hadron properties in the nuclear medium.

2 Experimental method

The general layout of the experimental setup is shown in Fig. 1. The experiment is performed at non-symmetric scattering angles of the final state protons in the coplanar quasi-free scattering geometry with a complete re-

Table 1: Solid target parameters

Target	Dimensions (mm)	Isotope concentration (%)
CH ₂	diameter x length	
	22x70	
	thickness x width x height	
⁶ Li	4.5x12x25	99.0
¹² C	4.0x18x70	98.9
²⁸ Si	6.0x25x70	99.9
⁴⁰ Ca	4.0x10x13	97.0

construction of the reaction kinematics. The measured secondary proton momenta K_1 , K_2 (kinetic energies T_1 , T_2) and the scattering angles Θ_1 , Θ_2 are used together with the proton beam energy T_0 to calculate nuclear proton separation energy $\Delta E = T_0 - T_1 - T_2$ and the residual nucleus momentum K_r for each $(p, 2p)$ event. In the impulse approximation, the K_r is equal to the momentum K of the nuclear proton before the interaction ($\mathbf{K}_r = -\mathbf{K}$).

External proton beam of the PNPI synchrocyclotron was focused onto the target TS of a two-arm spectrometer consisted of the magnetic spectrometers MAP and NES. The beam intensity was monitored by the scintillation telescope M1, M2, M3 and was about of $5 \cdot 10^{10}$ protons/(s·cm²).

The solid nuclear targets TS made from CH₂ (for the setup calibration), ⁶Li, ¹²C, ²⁸Si, ⁴⁰Ca (Table 1) and the universal cryogenic target with the liquid helium ⁴He (or with the liquid hydrogen for calibration) were used in the experiment [11, 20].

Cylindrical aluminium appendix of the cryogenic target had the dimensions: diameter - 65 mm, length - 70 mm, wall thickness - 0.1 mm. The

Table 2: Parameters of the magnetic spectrometers

Spectrometer	NES	MAP
Maximum particle momentum [GeV/c]	1.0	1.7
Axial trajectory radius ρ [m]	3.27	5.5
Deflection angle β , [deg]	37.2	24.0
Dispersion in the focal plane D_f , [mm/%]	24	22
Solid angle acceptance Ω , [sr]	$3.1 \cdot 10^{-3}$	$4.0 \cdot 10^{-4}$
Momentum acceptance $\Delta K/K$, [%]	8.0	8.0
Energy resolution (FWHM), [MeV]	~ 2.0	~ 1.5

diameter of the beam spot on the target was less than 15 mm. The spectrometers were used for registration of the secondary protons from the $(p, 2p)$ reaction in coincidence and for measurement of their momenta and outgoing angles. The polarization of these protons P_1 and P_2 , and the spin correlation parameters C_{ij} were measured by the polarimeters located in the region of focal planes of the spectrometers MAP and NES (Fig. 1). The left index of the C_{ij} , i (i is n or s'), and the right index j (j is n or s'') correspond to the forward scattered proton analysed by the MAP polarimeter and the recoil proton analysed by the NES polarimeter, respectively. The unit vector \mathbf{n} is perpendicular to the scattering plane of the reaction. Unit vectors \mathbf{s}' and \mathbf{s}'' are perpendicular to the vector \mathbf{n} and, the coordinate axes z' and z'' (Fig. 1) of the polarimeters.

The main parameters of the two-arm magnetic spectrometer and polarimeters are listed in Table 2 and Table 3, respectively.

Table 3: Polarimeter parameters

Polarimeter	NES	MAP
Carbon block thickness [mm]	79	199
Polar angular range [deg]	$6 \div 18$	$3 \div 16$
Average analyzing power	≥ 0.46	≥ 0.23
Efficiency [%]	~ 2	~ 5

The ΔE resolution of the spectrometer estimated from the elastic proton-proton scattering (Fig. 2, the left panel) with the 22-mm-thick cylindrical CH_2 target (see Table 1) was found to be about of 5 MeV (FWHM).

The track information from the proportional chambers of both polarimeters was used in the offline analysis to find the azimuthal ϕ_1 , ϕ_2 and polar θ_1 , θ_2 angles of the proton scattering from the analyzers A1, A2 for each $(p, 2p)$ event. In the case of absence of the accidental coincidence background (the case of the elastic proton-proton scattering) the polarization parameters could be found as [21]

$$P_{1,2} = \frac{2 \langle \cos \phi_{1,2} \rangle}{\langle A(\theta_{1,2}, K_{1,2}) \rangle}, \quad (1)$$

$$C_{nn} = \frac{4 \langle \cos \phi_1 \cos \phi_2 \rangle}{\langle A(\theta_1, K_1) \rangle \langle A(\theta_2, K_2) \rangle}, \quad (2)$$

$$C_{s,s''} = \frac{4 \langle \sin \phi_1 \sin \phi_2 \rangle}{\langle A(\theta_1, K_1) \rangle \langle A(\theta_2, K_2) \rangle}, \quad (3)$$

$$C_{ns''} = \frac{4 \langle \cos \phi_1 \sin \phi_2 \rangle}{\langle A(\theta_1, K_1) \rangle \langle A(\theta_2, K_2) \rangle}, \quad (4)$$

$$C_{s'n} = \frac{4 \langle \sin \phi_1 \cos \phi_2 \rangle}{\langle A(\theta_1, K_1) \rangle \langle A(\theta_2, K_2) \rangle}, \quad (5)$$

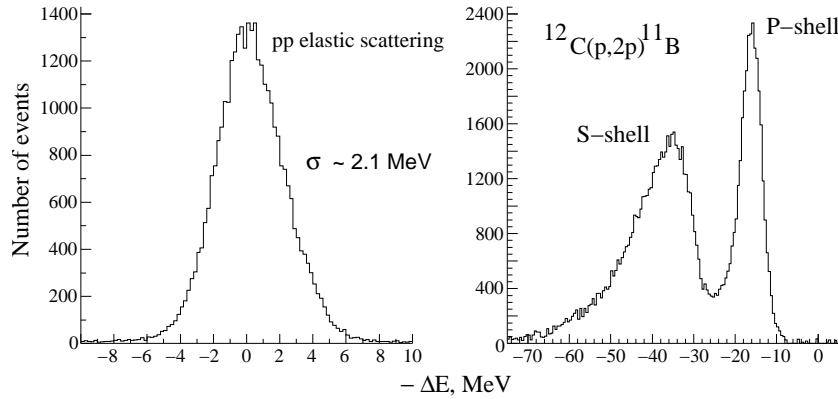


Figure 2: Proton separation energy spectra for the elastic pp scattering (the left panel) and for the $(p, 2p)$ reaction with the ^{12}C nucleus (the right panel). In the ^{12}C spectrum, the contribution from the accidental coincidence background was subtracted.

where averaging was made over a set of events within the working angular range of $\theta_{1,2}$ (see Table 3) for the polarimeters. $A(\theta_1, K_1)$ and $A(\theta_2, K_2)$, which were averaged over the same set of events, are the carbon analyzing power parameterized according to [22] and [23] for the MAP and NES polarimeter, respectively.

We estimated the polarization parameters by folding the theoretical functional shape of the azimuthal angular distribution into experimental one [13], using the CERNLIB MINUIT package [24] and likelihood χ^2 estimator [25]. This method permits to realize the control over χ^2 in the case the experimentally measured azimuthal distribution is distorted due to the instrumental problems.

The time difference (TOF) between the signals from the scintillation counters S2 and S4, was measured. It served to control the accidental coincidence background. The events from four neighboring proton beam bunches were

recorded. Three of them contained the background events only and were used in the offline analysis to estimate the background polarization parameters and the background contribution at the main bunch containing the correlated events [26]. The background polarization P_1 was found to be about 0.20-0.25 for all investigated nuclei. The polarization P_2 was less than 0.08. This value corresponds to the ^4He nucleus.

The recoil proton spectrometer NES was installed at a fixed angle $\Theta_2 \simeq 53.2^\circ$. At a given value of the S -shell mean binding energy of nucleus under investigation, the angular and momentum settings of the MAP spectrometer and the momentum setting of the NES spectrometer were chosen to get a kinematics of the $(p, 2p)$ reaction close to that of the elastic proton-proton scattering. In this kinematics, momentum K of the nuclear proton before the interaction is close to zero. At this condition, the counting rate of the S -shell proton knockout reaction should be maximal. In Fig. 2 (the right panel) and Fig. 3, the proton separation energy spectra for the reaction with the ^{12}C and ^{28}Si nuclei are shown. These spectra were obtained by subtracting the accidental coincidence background. As seen in Fig. 3, even at the preferable condition for the S -shell proton knockout process, the contribution from the scattering off the external shell protons for the heavy nucleus ^{28}Si is dominant. The number of the subtracted background events in the figure was approximately equal to the correlated ones in the ΔE region (between the dashed lines) used in offline analysis.

Measurements of the spin correlation parameters and even of the polarization in the $(p, 2p)$ reaction with heavy nuclei became possible due to the fast proportional chamber readout system, developed and produced at PNPI [18]. This electronics allowed us to collect the correlation events without distortion at a high rate of the accidental coincidence background.

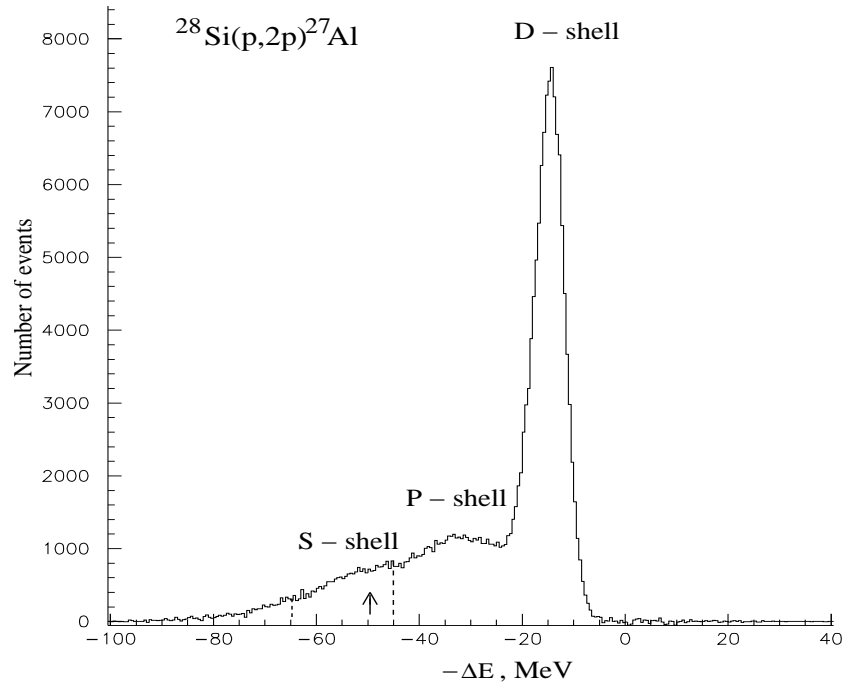


Figure 3: Proton separation energy spectrum for the reaction $^{28}\text{Si}(p,2p)^{27}\text{Al}$. The contribution from the accidental coincidence background was subtracted. The area between the vertical dashed lines was used for data analysis.

3 Results and discussion

In Fig. 4 and Table 4 in Appendix, the polarizations P_1 , P_2 in the $(p, 2p)$ reaction with the S -shell protons of the nuclei ${}^4\text{He}$, ${}^6\text{Li}$, ${}^{12}\text{C}$, ${}^{28}\text{Si}$, ${}^{40}\text{Ca}$ are plotted versus the S -shell proton binding energy E_s . For all nuclei (excluding ${}^4\text{He}$), the effective mean nuclear density $\bar{\rho}$, normalized on the saturation nuclear density $\rho_0 \approx 0.18 \text{ fm}^{-3}$, is given. The experimental data were obtained in the kinematical conditions when the nuclear S -shell proton before the interaction had momentum K close to zero. In this case the momentum $q=K_2$, transferred to a nucleus, depended weakly on a type of the nuclear target. The actual calculation of the effective mean nuclear density $\bar{\rho}$, which is determined by absorptions of the incident and both outgoing protons, was carried out following a procedure [15] using the computer code THREEDEE [17]. The potential model of a nucleus employed by the code is not correct for the ${}^4\text{He}$ nucleus. The calculated value of the $\bar{\rho}$ in this case is strongly unreliable [27]. The ${}^4\text{He}$ data should be excluded in comparing with theoretical models which differ from the PWIA.

The points (\circ) and (\bullet) in the figure correspond to the polarization P_1 and P_2 of the forward scattered protons at the angle $\Theta_1=21.0^\circ \div 25.08^\circ$ (with energy $T_1=745 \div 735 \text{ MeV}$) and the recoil protons scattered at the angle $\Theta_2 \simeq 53.2^\circ$ (with energy $T_2=205 \div 255 \text{ MeV}$). The points at the $E_s=0$ are the polarizations P_1 and P_2 in the elastic proton-proton scattering at the angles $\Theta_1=26.0^\circ$ and $\Theta_2=53.2^\circ$ ($\Theta_{cm}=62.25^\circ$). Note, that these pp data were obtained by a renormalization of the polarimeter analyzing power requiring that the measured polarization should match the value ($P_1=P_2=0.326$) given by the current phase-shift analysis SP07 [28]. The normalization coefficient was less than 1.06 for both polarimeters. This correction of the analyzing power

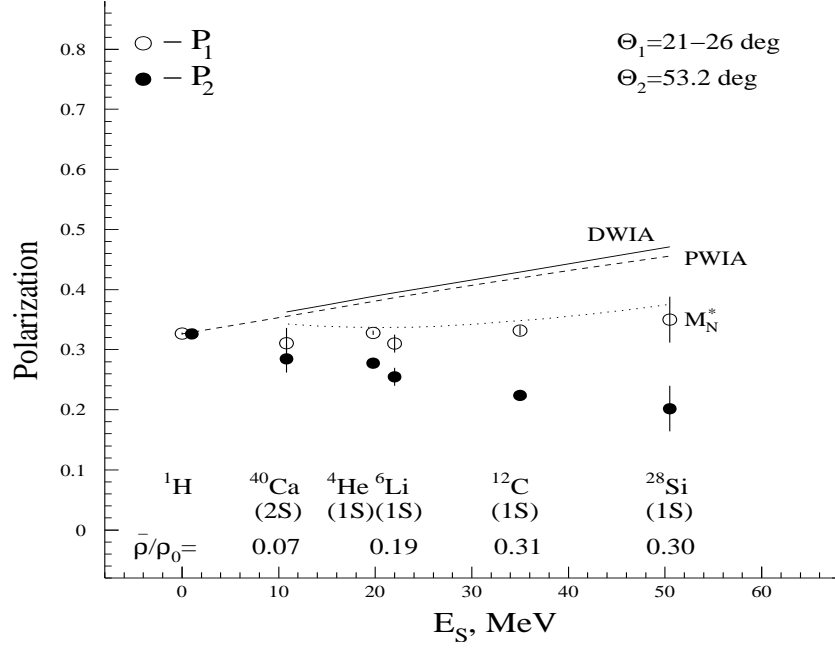


Figure 4: Polarizations P_1 and P_2 of the protons scattered at the angles Θ_1 (\circ) and $\Theta_2 \simeq 53.2^\circ$ (\bullet) in the $(p, 2p)$ reaction with the S -shell protons of nuclei at 1 GeV are plotted versus the S -shell mean binding energy E_s . For all nuclei (excluding ^4He), the effective mean nuclear density, $\bar{\rho}$ [15], in units of the saturation density ($\rho_0 = 0.18 \text{ fm}^{-3}$) is given. The points at $E_s = 0$ correspond to the elastic proton-proton scattering ($\Theta_1 = 26.0^\circ$). The dashed curve and the solid curve are the results of calculation in the PWIA and the DWIA, respectively, with the free NN interaction [17]. The dotted curve corresponds to the DWIA calculation with the relativistic effect taken into account [5].

was also made for the polarization data obtained in the $(p, 2p)$ experiment with nuclei.

In Fig. 4, the experimental data are compared with the results of the non-relativistic PWIA and DWIA calculations employing an on-shell factorized approximation. The final energy prescription was used for the calculations [29]. The dashed and solid curves correspond to the PWIA and DWIA calculations made using the computer code THREEDEE [17]. A global optical potential [30], parametrized in the relativistic framework and converted to the Shrödinger-equivalent form, was used to calculate the distorted waves of incident and outgoing protons in the case of DWIA. A conventional well-depth method was used to construct bound-state wave function. To calculate the secondary proton polarization, the THREEDEE code uses the 1986 Arndt NN phase-shift analysis (SP86) [31]. The results of the calculations presented in Fig. 4 were normalized to a ratio of the PWIA predictions obtained with the current phase-shift analysis SP07 [28] and the old one SP86. The value of the ratio $P(\text{SP07})/P(\text{SP86})$ was about of 1.025.

Because the difference between the P_1 and P_2 values in the DWIA calculations was found to be small, no more than 0.01, only the P_1 values obtained from the DWIA are plotted in Fig. 4. As seen in the figure, the difference between the PWIA and DWIA results is quite small. This result suggests that the distortion in the conventional non-relativistic framework does not play any essential role in the polarization for the employed kinematic conditions under consideration. The strong positive slope of the polarizations predicted by these calculations is caused by the kinematic effects of the binding energy of the struck proton. As seen in Fig. 4, there is a difference between the polarization P_1 calculated in the PWIA and that measured in the $(p, 2p)$ reaction with all nuclei under investigation.

In Fig. 4, the experimental data (excluding the ^4He data) are also compared with the theoretical calculations for the case when a relativistic effect, the distortion of the nucleon spinor, is taken into account (the M_N^* curve). The calculations were carried out in the Shrödinger equivalent form [10] using the THREEDEE code [17]. More specifically, these calculations consist of a non-relativistic DWIA calculations with the nucleon-nucleon t-matrix, that is modified in the nuclear potential following a procedure similar to that proposed by Horowitz and Iqbal [5]. In this approach a modified NN interaction in medium is assumed due to the effective nucleon mass (smaller than the free mass) which affects the Dirac spinors used in the calculations of the NN scattering matrix. A linear dependence of the effective mass of nucleons on the nuclear density was assumed in the calculations. As seen in the figure, this relativistic approach gives the results (the dotted curve) close to the experimental values of the forward scattered proton polarization P_1 at the large transferred momenta $q=3.2\div 3.7\text{ fm}^{-1}$ (see Table 4, Appendix). This indicates that the difference between the measured polarization P_1 and that calculated in the PWIA for the nuclei ^{40}Ca , ^6Li , ^{12}C , ^{28}Si is related to the value of the effective mean nuclear density $\bar{\rho}$. This observation provides an evidence for existing a nuclear medium effect. The Fig. 5 demonstrates that the relativistic approach (the dotted curve), mentined above, failed to reproduce the experimental polarization data for the ^{12}C nucleus at the transferred momentum q less than 3.4 fm^{-1} . The thick solid curve in the figure corresponds to the calculations in a fully relativistic model based on the distorted wave impulse approximation (RDWIA). In this model the four-component scattering and bound-state wave functions are governed by the relativistic Dirac equation [12]. Note, that in the full relativistic approach both real and imaginary components of the spin-orbit potential, which are crucial for describing polar-

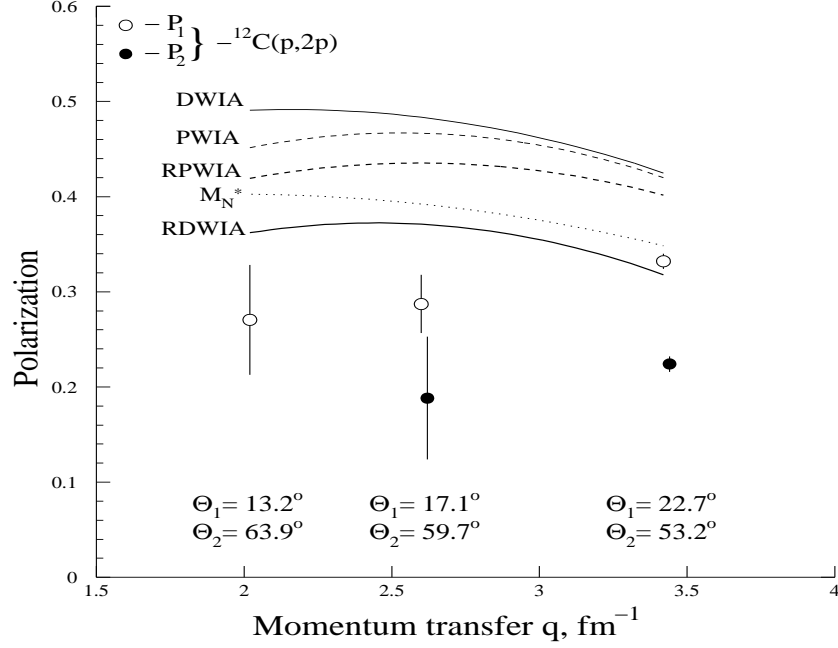


Figure 5: Angular dependence of the polarization for the $(p, 2p)$ reaction with 1S-shell proton of the ^{12}C nucleus. P_1 and P_2 are the polarizations of forward and recoil outgoing protons, respectively. The data are plotted as functions of the momentum q transferred to the nucleus. The thick dashed and solid curves are, respectively, the results of the full relativistic PWIA and DWIA calculations [12]. Identifications of the other curves are the same as those in Fig. 4. The data at $q < 3.4 \text{ fm}^{-1}$ are taken from [10].

ization phenomena, are directly related to the Lorentz properties of mesons mediating the strong nuclear force. This microscopic connection does not exist within the framework of the non-relativistic Schrödinger equation. In this case the spin-orbit interaction is usually introduced by hand and the interaction parameters are fitted to provide a good phenomenological description of the elastic scattering data. As seen from the figure, this relativistic approach also overestimates the experimental values of the P_1 polarization at the transferred momenta $q < 3.4 \text{ fm}^{-1}$. The difference may be related to another possible medium effect due to modifications of the exchanged meson masses and meson-nucleon coupling constants in the NN interaction. Krein et al. have shown in the relativistic Love-Franey model that these modifications cause significant changes in the spin observables [6]. A such type of modification was investigated in [12] using our early obtained experimental data on the polarization in the $(p, 2p)$ reaction with the ^{12}C nucleus measured in a wide range of the momentum transfer q [10]. Note, we essentially improved a statistical accuracy of the polarization measurement at the $q=3.4 \text{ fm}^{-1}$.

As seen in Fig. 4, there is a systematic difference between the P_1 and P_2 values, though they have the same values in the case of the elastic pp scattering. The Horowitz and Iqbal relativistic approach [5], considered above, also gives practically equal values of the polarizations. In Fig. 6, the relative difference $g = (P_2 - P_1)/P_1$ between the experimental values of the polarizations for all investigated nuclei is plotted versus the S-shell proton mean binding energy E_s . The dash-dotted line in the figure is the linear fit to the experimental data.

An origin of the stronger reduction of the polarization P_2 may be related to a manifestation of the recoil proton interaction with the short-lived two-

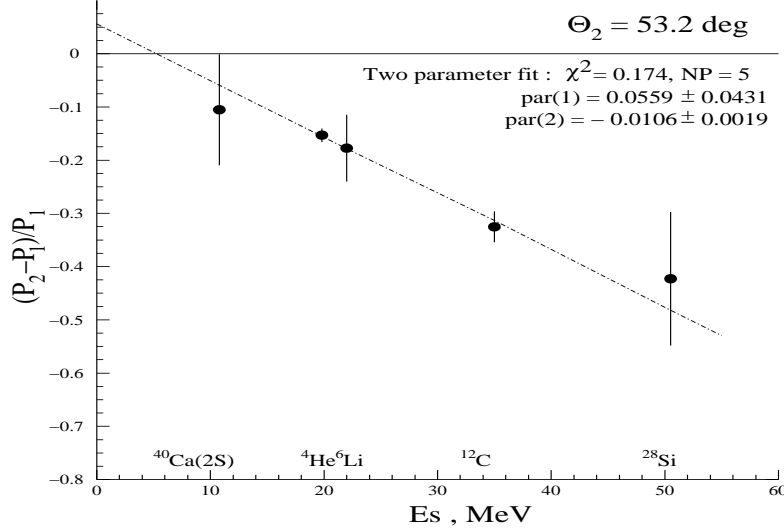


Figure 6: Relative difference $g=(P_2-P_1)/P_1$ of the measured polarizations P_2 , P_1 for all investigated nuclei. The dash-dotted curve is a linear fit to the experimental data.

nucleon or three-nucleon dense associations arose due to a fluctuation of the nucleon density in nuclear matter [32, 33]. The recoil S-shell proton with the momentum $K_2=q$ ($T_2 \sim 200$ MeV) and with the polarization $P_2 \simeq P_1$ elastically collides with the dense nucleon association. As a result, the S-shell proton of the association leaves a nucleus with the same momentum and, according to Pauli exclusion principle, with the opposite sign of the polarization $P_2 \simeq -P_1$. Taking into account a contribution from this depolarization mechanism, a probability of which is denoted as α , the averaged polarization of the recoil proton \bar{P}_2 is

$$\bar{P}_2 = (1 - \alpha)P_1 + \alpha(-P_1) = P_1(1 - 2\alpha), \quad (6)$$

and then the relative difference g between the polarizations \bar{P}_2 and P_1 is

$$g = \frac{(\bar{P}_2 - P_1)}{P_1} = -2\alpha. \quad (7)$$

The value of g extracted from the experimental data for the ^4He and ^{12}C nuclei (see Table 4 in Appendix) is equal to $g = -0.153 \pm 0.013$ and $g = -0.325 \pm 0.029$, respectively.

The spin correlation parameters C_{ij} in the reactions with the ^4He and ^{12}C nuclei were for the first time measured using an unpolarized 1 GeV proton beam. The results of the C_{ij} measurements are given in Fig. 7 (Table 5 in Appendix).

In Table 5, the measured mean values of the C_{ij} for the accidental coincidence background obtained in investigating the $(p, 2p)$ reaction with nuclei ^4He , ^{12}C and ^{28}Si are also presented. In Fig. 7, the dashed and dotted curves correspond to the PWIA calculations for the C_{nn} and $C_{s,s'}$. In these calculations, the current Arndt phase-shift analysis (SP07) was used [28]. The $C_{s,s'}$ parameter was found by taking into account its distortion in the magnetic fields of the MAP and NES spectrometers due to an anomalous proton magnetic moment [19]. The points at the mean binding energy value $E_s=0$ correspond to the elastic proton-proton scattering (see Table 6 in Appendix). These points in the figure are the averaging result of the pp experimental data obtained in 2008 and 2009 years when the nuclei ^4He and ^{12}C were investigated.

As seen in Fig. 7, the differences between the measured values of the C_{nn} and those calculated in the PWIA are within the statistical errors. The measured value of $C_{s,s'}$ in the elastic proton-proton scattering strongly differs from the SP07 prediction. This can be explained as a lack of the spin correlation parameter data from the elastic pp scattering experiments in the base of the current phase-shift analysis. Due to the parity conservation in the elastic proton-proton scattering, the spin correlation parameters $C_{ns''}$ and $C_{s'n}$ should be equal to 0. In Fig. 7, this is confirmed by the experimental data

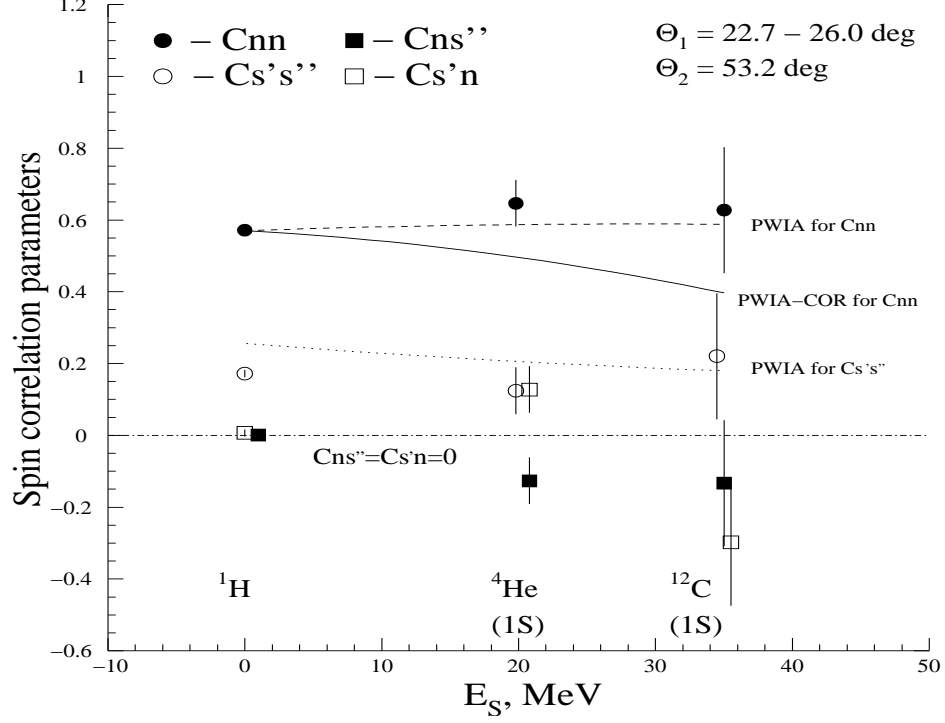


Figure 7: Spin correlation parameters C_{ij} in the $(p, 2p)$ reaction at 1 GeV with the S -shell protons of the ^4He and ^{12}C nuclei at the secondary proton scattering angles $\Theta_2=53.22^\circ$, $\Theta_1=24.21^\circ$ and $\Theta_2=53.22^\circ$, $\Theta_1=22.71^\circ$, respectively. The points at $E_s=0$ correspond to the averaged values of the polarization parameters in the elastic proton-proton scattering ($\Theta_1=26.0^\circ$, $\Theta_{cm}=62.25^\circ$), obtained in 2008-2009 years (Table 6 in Appendix). The dashed and dotted curves are the results of the PWIA calculation of the C_{nn} and $C_{s,s'}$ spin correlation parameters. The solid curve corresponds to the result of the PWIA-COR calculation taking into account the depolarization mechanism described in the text.

at the $E_s=0$. For a $(p, 2p)$ reaction with nuclei the parity in the pp system can be violated since there exists a residual nucleus in the knockout process. However, in this case, according to Pauli exclusion principle, a relation between the parameters in the center-of-mass pp interaction system $C_{ns''} = -C_{s'n}$ should be valid [34]. This relation can be violated in the laboratory system because of a distortion of the parameters by the magnetic fields of both spectrometers.

In Fig. 7, the experimental C_{nn} data for the ^4He and ^{12}C nuclei are also analysed in the framework of the plane wave impulse approximation with the correction to a contribution from the depolarisation mechanism PWIA-COR related to the mentioned above recoil-proton elastic interaction with the dense nucleon associations in a nucleus (the solid curve). The averaged value of the spin correlation parameter \bar{C}_{nn} in the PWIA-COR model was calculated using equation similar to Eq. (6) for the recoil proton polarization \bar{P}_2 :

$$\bar{C}_{nn} = (1 - \alpha)C_{nn} + \alpha(-C_{nn}) = C_{nn}(1 - 2\alpha) = C_{nn}(1 + g), \quad (8)$$

where the C_{nn} is the result of the PWIA calculation (the dashed curve) and the $g < 0$ is the relative difference of the P_2 and P_1 experimental polarization values (Eq. (7)), calculated above for the ^4He and ^{12}C nuclei. As seen in Fig. 7, the C_{nn} experimental values for the nuclei exceed those calculated in the PWIA-COR. Therefore, the nuclear medium increases the C_{nn} parameter value in the $(p, 2p)$ reaction in comparison with the elastic pp scattering. On the contrary, as shown above, the NN -scattering amplitudes are modified in nuclear matter so that the polarization in the reaction is less than that in the elastic pp interaction.

4 Summary

The polarizations P_1 and P_2 of both secondary protons from the $(p, 2p)$ reaction with the $1S$ -shell protons of the nuclei ${}^4\text{He}$, ${}^6\text{Li}$, ${}^{12}\text{C}$, ${}^{28}\text{Si}$ and with $2S$ -shell protons of the ${}^{40}\text{Ca}$ nucleus were measured at 1 GeV energy of unpolarized proton beam. The spin correlation parameters C_{ij} in the reaction with the nuclei ${}^4\text{He}$ and ${}^{12}\text{C}$ were for the first time obtained. The experiments were performed at the non-symmetric scattering angles of the final state protons $\Theta_1=21^\circ\div 25^\circ$ and $\Theta_2 \simeq 53.2^\circ$ in the coplanar quasi-free scattering geometry with a complete reconstruction of the reaction kinematics. The measurements were done in the kinematical conditions when the nuclear S -shell proton (before the interaction) had the momentum K close to zero. In this case the transferred momentum q , which is equal to the recoil proton momentum K_2 , depended weakly on a type of the nuclear target ($q=3.2\div 3.7$ fm $^{-1}$).

The observed reduction of the polarization P_1 of the forward scattered protons in the reaction with the nuclei ${}^6\text{Li}$, ${}^{12}\text{C}$, ${}^{28}\text{Si}$ and ${}^{40}\text{Ca}$ in comparison with that calculated in the framework of the PWIA and DWIA depends on the effective mean nuclear density. The calculations in the DWIA, in the framework of which a modification of nucleon Dirac spinor is taken into account, reproduce the magnitude of the reduction well. The inessential difference between the non-relativistic PWIA and DWIA calculations points out to a small depolarization of the secondary protons because of the proton-nucleon rescatterings in a nucleus. All these facts indicate a modification of the proton-proton scattering matrix in the nuclear medium.

The experiment with the ${}^4\text{He}$ nucleus shows that the magnitude of the P_1 polarization reduction in the light nuclei at least ($A<12$) is also determined

by the mean binding energy of the S -shell proton of a nucleus. Another significance of the experiment with the ${}^4\text{He}$ nucleus is the possibility to see the medium effect without any contribution from the multi-step processes. These processes can take place when there are nucleons of outer shells as in other nuclei. The experiment also points out that the multi-step processes are not the main origin of the observed negative difference of the polarizations of the recoil proton P_2 and the forward scattered proton P_1 .

The systematic relative difference between the P_2 and P_1 polarizations was observed in investigating the $(p, 2p)$ reaction with nuclei. This effect depends likely on the value of the mean binding energy E_s of the S -shell protons. An origin of the effect may be related to the depolarization mechanism of the recoil proton interaction with the short-lived dense nucleon associations in a nucleus. This depolarization mechanism decreases the value of the spin correlation parameter C_{nn} in comparison with that calculated in the PWIA. In this reason, the C_{nn} experimental values for the nuclei ${}^4\text{He}$ and ${}^{12}\text{C}$ exceed those calculated in the PWIA with a contribution from the mechanism included. Therefore, the nuclear medium affects the C_{nn} parameter in the $(p, 2p)$ reaction increasing its value in comparison with that in the elastic pp scattering. On the contrary, the NN scattering amplitudes are modified in nuclear matter so that the polarization in the $(p, 2p)$ reaction is less than that in the elastic pp interaction.

5 Acknowledgments

This work is partly supported by the Grant of President of the Russian Federation for Scientific School, Grant-3383.2010.2.

The authors are grateful to PNPI 1 GeV proton accelerator staff for stable beam operation. We thank members of PNPI HEP Radio-electronics Laboratory for providing the CROS-3 proportional chamber readout system.

Also, the authors would like to express their gratitude to A.A. Vorobyov and S.L. Belostotski for their support and fruitful discussions.

6 Appendix: Experimental results

Table 4: Secondary proton polarizations P_1 and P_2 in the $(p, 2p)$ reaction at 1 GeV with the S -shell protons of nucleus at lab. angles Θ_1 and Θ_2

Nucleus	Θ_1 deg.	Θ_2 deg.	T_1 MeV	T_2 MeV	q fm^{-1}	P_1	P_2	$\bar{\rho}/\rho_0$
^4He (1S)	24.21	53.22	738	242	3.6	.328 \pm .003	.278 \pm .003	
^6Li (1S)	24.0	53.25	739	239	3.6	.310 \pm .015	.255 \pm .015	.19
^{12}C (1S)	22.71	53.22	746	219	3.4	.332 \pm .008	.224 \pm .008	.31
^{28}Si (1S)	21.0	53.22	746	204	3.2	.350 \pm .038	.202 \pm .038	.30
^{40}Ca (2S)	25.08	53.15	734	255	3.7	.311 \pm .025	.285 \pm .023	.07

Table 5: Spin correlation parameters C_{ij} in the $(p, 2p)$ reaction at 1 GeV with the S -shell protons of the ^4He and ^{12}C nuclei at lab. angles Θ_1 and $\Theta_2=53.22^\circ$. The line "Background" corresponds to the measured mean values of the C_{ij} for the accidental coincidence background, obtained in investigating the reaction with the nuclei ^4He , ^{12}C and ^{28}Si

Nucleus	Θ_1 deg.	C_{nn}	$C_{s,s'}$	$C_{ns'}$	$C_{s,n}$
^4He	24.21	$.647 \pm .065$	$.124 \pm .065$	$-.126 \pm .065$	$.128 \pm .065$
^{12}C	22.71	$.628 \pm .176$	$.220 \pm .176$	$-.133 \pm .176$	$-.298 \pm .176$
Background		$-.006 \pm .019$	$.01 \pm .019$	$.016 \pm .019$	$.001 \pm .019$

Table 6: Spin correlation parameters C_{ij} in the elastic proton-proton scattering at 1 GeV at lab. angles $\Theta_1=26.0^\circ$ and $\Theta_2=53.22^\circ$ ($\Theta_{cm}=62.25^\circ$). Results of 2008-2010 years. The current phase-shift analysis predicts the C_{nn} value of 0.57. The statistical errors of the polarization P_1 and P_2 measurements are given. The systematic uncertainty in the polarization measurements was about of ± 0.004 and ± 0.0025 for the MAP and NES polarimeters, respectively [13].

Year	C_{nn}	$C_{s,s'}$	$C_{ns'}$	$C_{s,n}$	δP_1	δP_2
2008	$.557 \pm .013$	$.185 \pm .013$	$.010 \pm .013$	$-.003 \pm .013$.0008	.0007
2009	$.589 \pm .015$	$.154 \pm .015$	$-.012 \pm .015$	$.020 \pm .015$.0011	.0007
2010	$.575 \pm .030$	$.176 \pm .030$	$-.029 \pm .030$	$-.003 \pm .030$.0021	.0015

References

- [1] G. E. Braun and M. Rho, Phys. Lett. **66** (1991) 2720 .
- [2] R. J. Furnstahl *et al.*, Phys. Rev. C **46**(1992) 1507.
- [3] T. Hatsuda, Nucl. Phys. A **544**(1992) 27 .
- [4] B. D. Serot and J. D. Walecka, in *Advances in Nucl. Phys.*, edited by J. W. Negele and E. Vogt (Plenum Press, New York, 1986), Vol. 16, p. 116.
- [5] C. J. Horowitz and M. J. Iqbal, Phys. Rev. C **33**(1986) 2059.
- [6] G. Krein, Th. A. J. Maris, B. B. Rodrigues and E. A. Veit, Phys. Rev. C **51**(1995) 2646.
- [7] O. V. Miklukho *et al.*, Phys. Atom. Nucl. **63**(2000) 824 .
- [8] O. V. Miklukho *et al.*, Nucl.Phys. A **683** (2001) 145.
- [9] O. V. Miklukho *et al.*, Czech. J. Phys. **52** Suppl. C (2002) 293.
- [10] V. A. Andreev *et al.*, Phys. Rev. C **69**,(2004) 024604.
- [11] O. V. Miklukho *et al.*, Phys. Atom. Nucl. **69**(2006) 474.
- [12] G. C. Hillhouse and T. Noro, Phys. Rev. C **74**(2006) 064608.
- [13] O. V. Miklukho *et al.*, Phys. Atom. Nucl. **73**(2010) 927.
- [14] G. Jacob *et al.*, Nucl. Phys. A **257**(1976) 517.
- [15] K. Hatanaka *et al.*, Phys. Rev. Lett. **78**(1997) 1014.

- [16] T. Noro *et al.*, Nucl. Phys. B **633-664**(2000) 517 .
- [17] N. S. Chant and P. G. Roos, Phys. Rev. C **27**(1983) 1060.
- [18] N. F. Bondar *et al.* in *PNPI Main Scientific Activities 2002-2006*. PNPI, Gatchina (2007) 334.
- [19] W. O. Lock and D. F. Measday, *Intermediate-Energy Nuclear Physics*. (Methuen, London, 1970; Atomizdat, Moscow, 1973).
- [20] L. Kotchenda *et al.*, Preprint PNPI-2816, Gatchina (2009).
- [21] O. Ya. Fedorov, Preprint PNPI-2432, Gatchina (2001) [in Russian].
- [22] O. Ya. Fedorov, Preprint LNPI-484, Gatchina (1979) [in Russian].
- [23] G. Waters *et al.*, Nucl. Instrum. Methods **153**(1978) 401.
- [24] F. James, MINUIT, CERN Program Library Long Writeup D506 , Geneva (1998).
- [25] S. Baker and R. Cousins, Nucl. Instrum. Methods **221**(1984) 437.
- [26] A. Yu. Kisselev, *Investigation of the polarization in $(p,2p)$ reaction with S -shell protons of nuclei ${}^6\text{Li}$, ${}^{12}\text{C}$, ${}^{28}\text{Si}$, ${}^{40}\text{Ca}$ at 1 GeV*. PhD Thesis, PNPI (2012) [in Russian].
- [27] O. V. Miklukho *et al.* in *PNPI Main Scientific Activities 2002-2006*. PNPI, Gatchina, (2007) 184.
- [28] R. A. Arndt *et al.*, arXiv: 0706.2195v2 [nucl-th], 16 P. (2007) or <http://gwdac.phys.gwn.edu>.
- [29] W. T. H. van Oers *et al.*, Phys. Rev. C **25**(1982) 390.

- [30] E. D. Cooper, S. Hama, B. C. Clark and R. L. Mercer, Phys. Rev. C **47**(1993) 297.
- [31] J. Bystricky, F. Lehar, and P. Winternitz, J. Phys.(Paris) **39**(1978) 1.
- [32] D. I. Blokhintsev, Sov. J. ZhETF **33**(1957) 1295 [in Russian].
- [33] K. S. Egiyan *et al.*, Phys. Rev. Lett. **96**(2006) 082501.
- [34] H. Faissner, *Polarisierte Nucleonen I: Polarisation durch streuung*. Springer, 167 P. (1959).